

1 **The Landscape of Sex- and APOE Genotype-Specific Transcriptional Changes in**
2 **Alzheimer's Disease at the Single Cell Level**

3
4 Gefei Yu^{1,2}, Abigail Thorpe^{1,2}, Qi Zeng^{1,2}, Ermeng Wang^{1,2}, Dongming Cai^{3,4,5}, Minghui
5 Wang^{1,2,6*}, Bin Zhang^{1,2,6,7*}

6
7 ¹Department of Genetics and Genomic Sciences, Icahn School of Medicine at Mount Sinai, One
8 Gustave L. Levy Place, New York, NY, 10029, USA.

9 ²Mount Sinai Center for Transformative Disease Modeling, Icahn School of Medicine at Mount
10 Sinai, One Gustave L. Levy Place, New York, NY, 10029, USA.

11 ³Department of Neurology, University of Minnesota, Minneapolis, MN 55455

12 ⁴N. Bud Grossman Center for Memory Research and Care, University of Minnesota, Minneapolis,
13 MN 55455

14 ⁵Geriatric Research Education & Clinical Center (GRECC), Minneapolis VA Health Care System,
15 Minneapolis, MN 55417

16 ⁶Icahn Genomics Institute, One Gustave L. Levy Place, New York, NY, 10029, USA.

17 ⁷Department of Pharmacological Sciences, Icahn School of Medicine at Mount Sinai, One Gustave
18 L. Levy Place, New York, NY, 10029, USA.

19 *To whom correspondence should be addressed:

20 Bin Zhang, PhD

21 Email: bin.zhang@mssm.edu

22 Minghui Wang, PhD

23 Email: minghui.wang@mssm.edu

24

25

26

27

28

29

30 **Abstract**
31
32 Alzheimer's disease (AD) is the most common form of dementia, with approximately two-thirds
33 of AD patients are females. Basic and clinical research studies show evidence supporting sex-
34 specific differences contributing to the complexity of AD. There is also strong evidence supporting
35 sex-specific interaction between the primary genetic risk factor of AD, *APOE4* and AD-associated
36 neurodegenerative processes. Recent studies by us and others have identified sex and/or *APOE4*
37 specific differentially expressed genes in AD based on the bulk tissue RNA-sequencing data of
38 postmortem human brain samples in AD. However, there lacks a comprehensive investigation of
39 the interplay between sex and *APOE* genotypes at the single cell level. In the current study, we
40 systematically explore sex and *APOE* genotype differences in single cell transcriptomics in AD.
41 Our work provides a comprehensive overview of sex and *APOE* genotype-specific transcriptomic
42 changes across 54 high-resolution cell types in AD and highlights individual genes and brain cell
43 types that show significant differences between sexes and *APOE* genotypes. This study lays the
44 groundwork for exploring the complex molecular mechanisms of AD and will inform the
45 development of effective sex- and *APOE*-stratified interventions for AD.

46

47 **INTRODUCTION**

48
49 Alzheimer's disease (AD) is the most prevalent neurodegenerative disorder of aging ¹, with
50 approximately two-thirds of AD patients are females ². There are conflicting literature reports
51 regarding AD incidents among males and females with some suggesting a higher AD incidence in
52 females than males and others suggesting no differences ³⁻⁷. Evidence from basic and clinical
53 research studies supports sex-specific differences contributing to the complexity of AD. For
54 example, sex-biased changes in brain structures and connectome have been demonstrated in AD
55 subjects using various neuroimaging modalities. It was found that the rates of brain atrophy in
56 females were 1-1.5% faster than those in males, most prominently seen in the MCI group with a
57 1% increase in atrophic rates and 2% in ventricular expansion ⁸. Sex-specific brain region atrophy
58 have also been reported ⁹. Moreover, a significantly higher reduction of hippocampal integrity in
59 female AD subjects was reported when compared to male subjects with Magnetic Resonance
60 Imaging studies of the Minimal Interval Resonance Imaging in AD database ¹⁰.

61 There is strong evidence supporting sex-specific interaction between the primary genetic
62 risk factor of AD, *APOE4* ¹¹ and AD-associated neurodegenerative processes ^{12, 13}. The sex-
63 specific association between *APOE4* and tau has been reported ^{14, 15}. Furthermore, studies suggest
64 a stronger association of *APOE4* with cortical thinning, volume loss, brain connectivity and hypo-
65 metabolism in AD females than males ¹⁶⁻¹⁸. Moreover, stronger associations of *APOE4* with
66 cognitive impairment, memory decline, and neuropsychiatric symptoms of AD in females were
67 reported ^{19, 20}. On the other hand, male-specific associations with cerebral amyloid angiopathy
68 (CAA) and microbleed in AD have been reported ²¹. Even so, little has been done to understand
69 the interplay between *APOE* and sex in ageing and AD.

70 Recently, we systematically identified sex and *APOE4* specific differentially expressed
71 genes in AD²² based on the bulk tissue RNA-sequencing data of postmortem human brain samples
72 from the Mount Sinai Brain Bank (MSBB) cohort ²³ and the Religious Orders Study and Rush
73 Memory and Aging Project (ROSMAP) cohort ²⁴. We further developed sex-specific gene
74 network models of AD to predict sex specific driver genes of AD and subsequently validated
75 *LRP10* (lipoprotein receptor related protein 10) as a female-specific driver of AD pathogenesis²².

76 In the current study, we further investigate the interplay between sex and *APOE* in AD at
77 single cell level through differential gene expression analysis of single-nucleus RNA sequencing
78 data. The findings not only provide a comprehensive overview of sex and *APOE* genotype-specific
79 transcriptomic changes across 54 high-resolution cell types in AD but also highlight individual
80 genes and brain cell types that show significant differences between sexes and *APOE* genotypes.
81 This study lays the groundwork for exploring the complex molecular mechanisms of AD and will
82 inform the development of effective sex- and *APOE*-stratified interventions for AD.

83
84 **RESULTS**

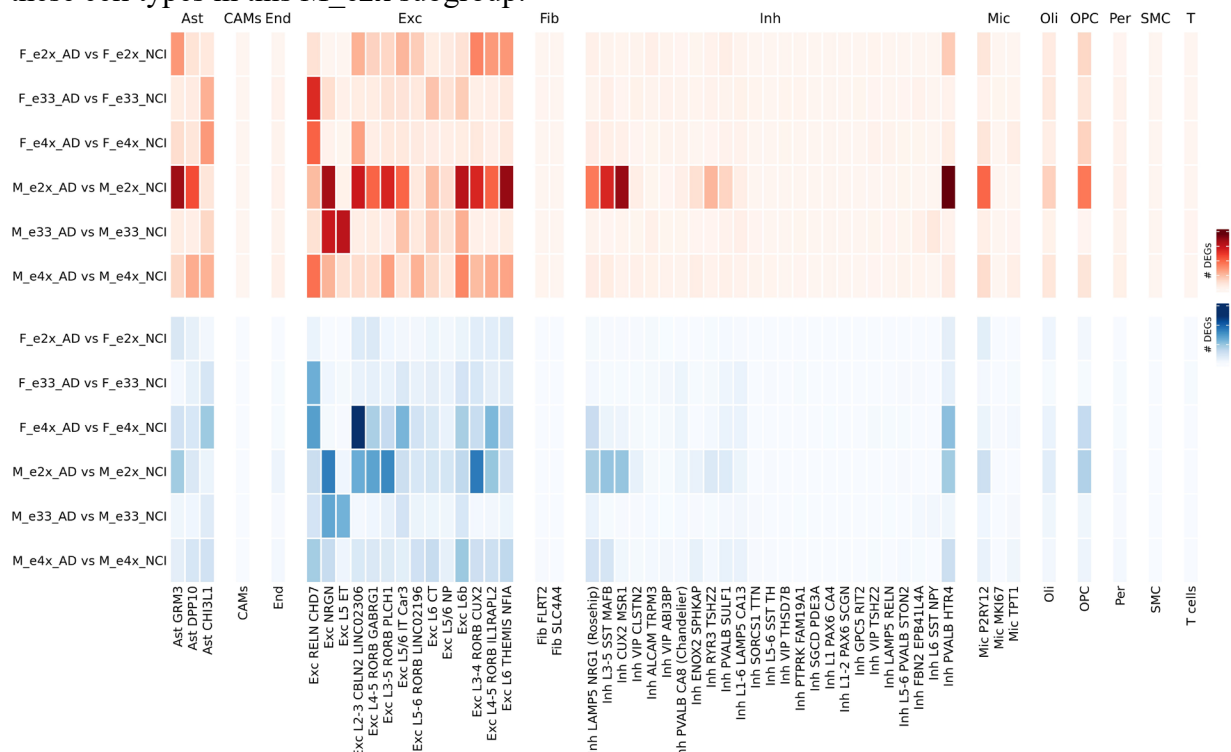
85
86 We leveraged a single-nucleus RNA sequencing (snRNA-seq) dataset which was generated from
87 postmortem brain tissues of subjects with or without dementia by Mathys et al.²⁵. The dataset
88 profiled 2,359,994 nuclei from 427 prefrontal cortex brain samples, including 215 female and 212
89 male donors. Disease status was categorized using the final consensus cognitive diagnosis score
90 (cogdx), where 1 = no cognitive impairment (NCI), 2 = mild cognitive impairment (MCI), 4 =
91 Alzheimer's disease (AD), and 3, 5, 6 were categorized as other dementia. For this study, we
92 focused solely on NCI (n = 146) and AD (n = 144) samples. To investigate the impact of *APOE*

genotypes, we grouped participants as follows: *APOE* e22 and e23 were categorized as *APOE* e2 carriers (e2x; n = 58), e33 remained as e33 (n = 252), and e34 and e44 were classified as *APOE* e4 carriers (e4x; n=105). *APOE* e24 carriers were excluded from the analysis due to the controversial nature of their association with disease risk.

We utilized the 54 cell clusters identified in the original study²⁵: 14 excitatory neuron clusters, 25 inhibitory neuron clusters, 1 oligodendrocyte cluster, 1 oligodendrocyte precursor cell cluster, 3 astrocyte cell clusters, 3 microglia cell clusters, 1 central nervous system (CNS)-associated macrophage (CAM) cluster, 1 T cell cluster, 1 endothelial cells (End) cluster, 1 smooth muscle cell (SMC) cluster, 2 fibroblasts (Fib) clusters, and 1 pericytes (Per) cell cluster.

Cell type specific gene expression changes in AD in each sex-*APOE* subgroup

To investigate the transcriptional changes associated with AD in each *APOE* genotype (e2x, e33, and e4x) or sex group (female (F) and male (M)), we performed cell-cluster-specific differential gene expression (DEG) analysis across six stratified comparisons. For each sex-*APOE* group (F_e2x, F_e33, F_e4x, M_e2x, M_e33, and M_e4x), we compared gene expression profiles of the individuals with AD with those with no cognitive impairment (NCI). This stratification allowed us to capture genotype- and sex-specific transcriptional alterations in AD in each cell cluster, offering a detailed view of how these factors shape the molecular landscape in AD. The numbers of up-regulated and down-regulated DEGs identified in these comparisons are shown in **Figure 1**. The distribution of DEGs across cell clusters revealed distinct patterns. Excitatory neurons exhibited a substantial number of DEGs in almost all sex-*APOE* groups. Notably, the AD males with *APOE* e2 carriers (M_e2x) had the highest number of DEGs compared to other sex-*APOE* groups, particularly in the excitatory neuron (Exc), inhibitory neuron (Inh), OPC, and microglia (Mic) clusters. This suggests a potentially heightened transcriptional response to AD in these cell types in this M_e2x subgroup.



119 **Figure 1. Heatmap showing the number of differentially expressed genes (DEGs) between**
120 **AD samples and NCI samples within each sex-APOE group (F_e2x, F_e33, F_e4x, M_e2x,**
121 **M_e33, M_e4x) across all the 54 cell clusters.** The upper heatmap represents the number of
122 upregulated DEGs (red), while the lower heatmap depicts the number of downregulated DEGs
123 (blue). Each row corresponds to a specific comparison, and each column represents a distinct cell
124 cluster.

125

126 **Comparative study of transcriptional signatures between different sex-APOE subgroups**

127 To further explore transcriptional changes in AD, we conducted a series of pairwise
128 comparisons to identify the overlap and divergence in differentially expressed genes (DEGs)
129 across APOE genotypes and between sexes. These analyses aimed to identify both shared and
130 unique transcriptional responses among subgroups, offering insights into how genotype and sex
131 interact to influence molecular changes in AD in each brain cell type.

132

133 **Comparison of transcriptional signatures across *APOE* genotypes in females and males**

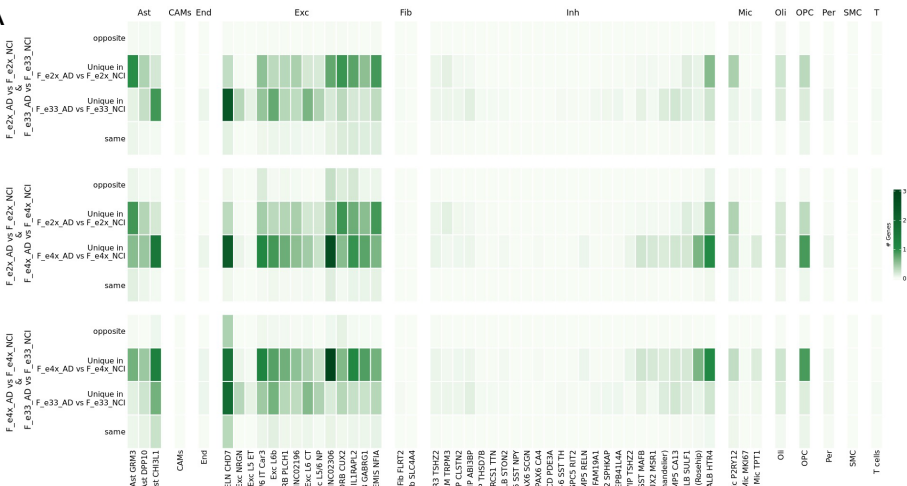
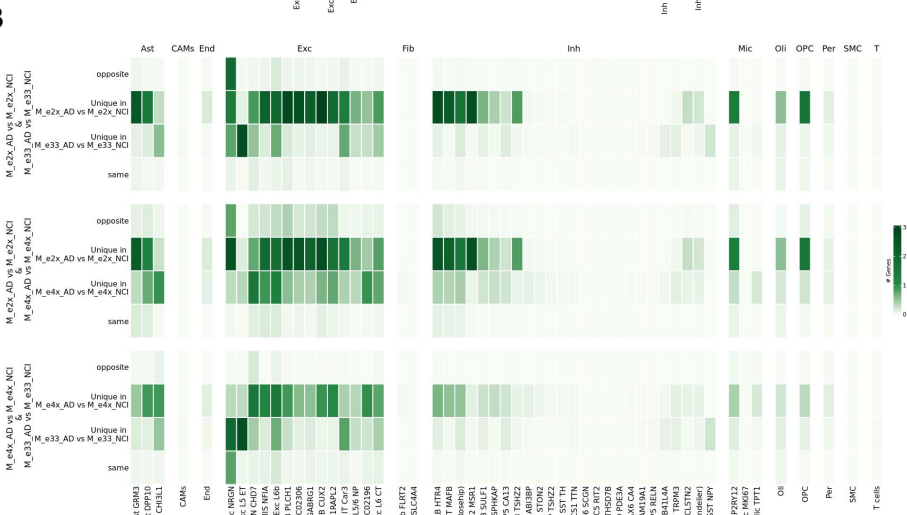
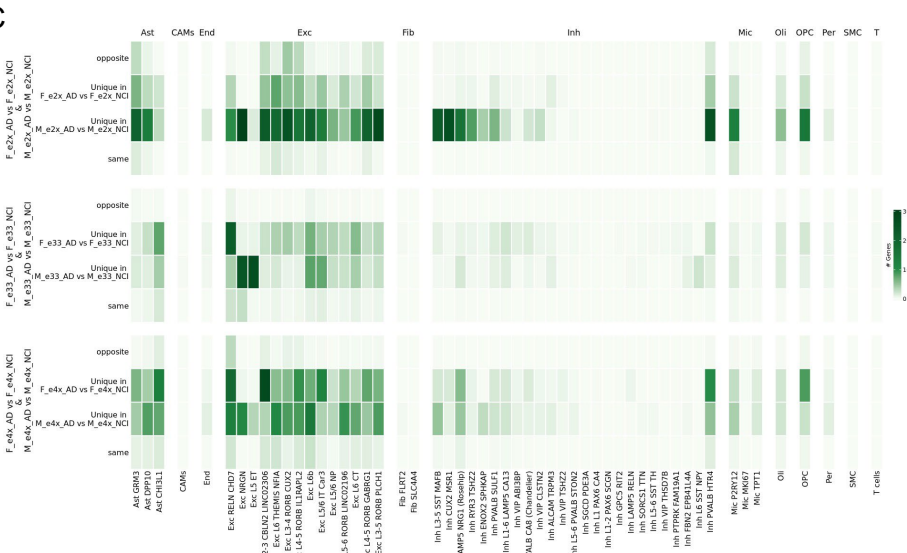
134 We first compared the DEG signatures between females across *APOE* genotypes (F_e2x,
135 F_e33, and F_e4x) to explore *APOE* genotype-specific transcriptional patterns in female (**Fig. 2A**).
136 Comparisons included 1). F_e2x_AD vs. F_e2x_NCI and F_e33_AD vs. F_e33_NCI, 2).
137 F_e2x_AD vs. F_e2x_NCI and F_e4x_AD vs. F_e4x_NCI, and 3). F_e4x_AD vs. F_e4x_NCI and
138 F_e33_AD vs. F_e33_NCI. Notably, *APOE* e4 carriers showed more distinct transcriptional
139 changes than the other genotypes, highlighting the unique impact of the e4 genotype on AD
140 females.

141 The same analysis was applied to the male *APOE* groups (M_e2x, M_e33, and M_e4x),
142 including 1) M_e2x_AD vs. M_e2x_NCI and M_e33_AD vs. M_e33_NCI, 2) M_e2x_AD vs.
143 M_e2x_NCI and M_e4x_AD vs. M_e4x_NCI, and 3) M_e4x_AD vs. M_e4x_NCI and
144 M_e33_AD vs. M_e33_NCI. As shown in **Fig. 2B**, *APOE* e2 carriers exhibited a more pronounced
145 transcriptional divergence from other genotypes, particularly within excitatory neurons, inhibitory
146 neurons and astrocytes. This pattern suggests that *APOE* e2 carriers in males may activate certain
147 distinct transcriptional programs in AD, with greater cell-type specificity than observed in females.

148

149 **Comparison Across Sexes Within Each *APOE* Genotype**

150 Lastly, we examined the overlap and difference in DEGs between sexes for each *APOE*
151 genotype (**Fig. 2C**). Comparisons included 1) F_e2x_AD vs. F_e2x_NCI and M_e2x_AD vs.
152 M_e2x_NCI, 2) F_e33_AD vs. F_e33_NCI and M_e33_AD vs. M_e33_NCI, and 3) F_e4x_AD
153 vs. F_e4x_NCI and M_e4x_AD vs. M_e4x_NCI. The results, visualized in **Figure 2C**,
154 demonstrate significant sex-specific transcriptional differences in *APOE* e2 and *APOE* e4
155 genotypes. *APOE* e33 groups (F_e33_AD vs. F_e33_NCI and M_e33_AD vs. M_e33_NCI) had
156 relatively fewer transcriptional differences between sexes across most cell clusters compared to
157 e2x or e4x carriers. This observation aligns with the known biological role of the e33 genotype,
158 which is generally considered neutral in terms of AD risk, in contrast to e2, which is protective,
159 and e4, which is associated with heightened risk. The limited sex-specific divergence in e33
160 carriers suggests a more stable transcriptional landscape, potentially reflecting the absence of
161 strong protective or risk-associated pressures on gene expression within this genotype.

A**B****C**

163 **Figure 2. Comparative study of transcriptional signatures between different sex-APOE**
164 **subgroups.** A) Heatmap illustrating the overlap, unique, and opposite differentially expressed
165 genes (DEGs) between female APOE groups (F_e2x, F_e33, and F_e4x) across cell clusters. Each
166 row corresponds to a specific comparison, including: 1). F_e2x_AD vs. F_e2x_NCI and
167 F_e33_AD vs. F_e33_NCI, 2). F_e2x_AD vs. F_e2x_NCI and F_e4x_AD vs. F_e4x_NCI, and 3).
168 F_e4x_AD vs. F_e4x_NCI and F_e33_AD vs. F_e33_NCI. B) Heatmap illustrating the overlap,
169 unique, and opposite differentially expressed genes (DEGs) between male APOE groups (M_e2x,
170 M_e33, and M_e4x) across cell clusters. Each row corresponds to a specific comparison, including:
171 1). M_e2x_AD vs. M_e2x_NCI and M_e33_AD vs. M_e33_NCI, 2). M_e2x_AD vs. M_e2x_NCI
172 and M_e4x_AD vs. M_e4x_NCI, and 3). M_e4x_AD vs. M_e4x_NCI and M_e33_AD vs.
173 M_e33_NCI. C) Heatmap illustrating the overlap, unique, and opposite differentially expressed
174 genes (DEGs) between males and females within each APOE genotype (e2x, e33, and e4x) across
175 cell clusters. Each row corresponds to a specific comparison, including: 1). F_e2x_AD vs.
176 F_e2x_NCI and M_e2x_AD vs. M_e2x_NCI, 2). F_e33_AD vs. F_e33_NCI and M_e33_AD vs.
177 M_e33_NCI, and 3). F_e4x_AD vs. F_e4x_NCI and M_e4x_AD vs. M_e4x_NCI.

178

179

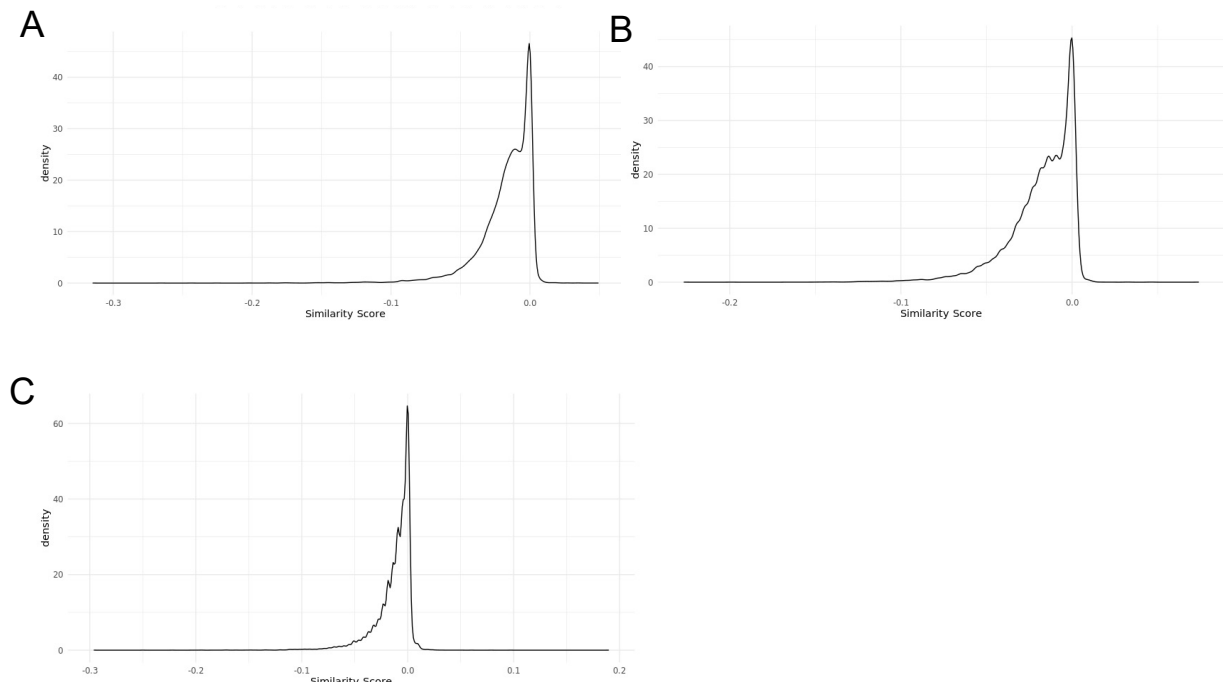
180 **Similarity measures reveal shared and divergent transcriptional changes across sexes and**
181 **APOE genotypes in AD**

182 To quantitatively evaluate the similarity of differential expression patterns across sexes and
183 APOE genotypes, we developed a new similarity measure for ternary vectors, termed as Zhang-
184 Yu similarity measure (see **the Materials and Methods section** for the details). Each element in
185 a ternary vector represents the differential expression status of a gene from a specific comparison
186 with -1 standing for significant down-regulation, 0 for no significant change, and +1 for significant
187 upregulation. The Zhang-Yu similarity measure quantitatively assesses the overlap, divergence,
188 and directional consistency of gene expression changes across comparisons. Higher similarity
189 scores indicate greater similarity while lower scores reflect divergence.

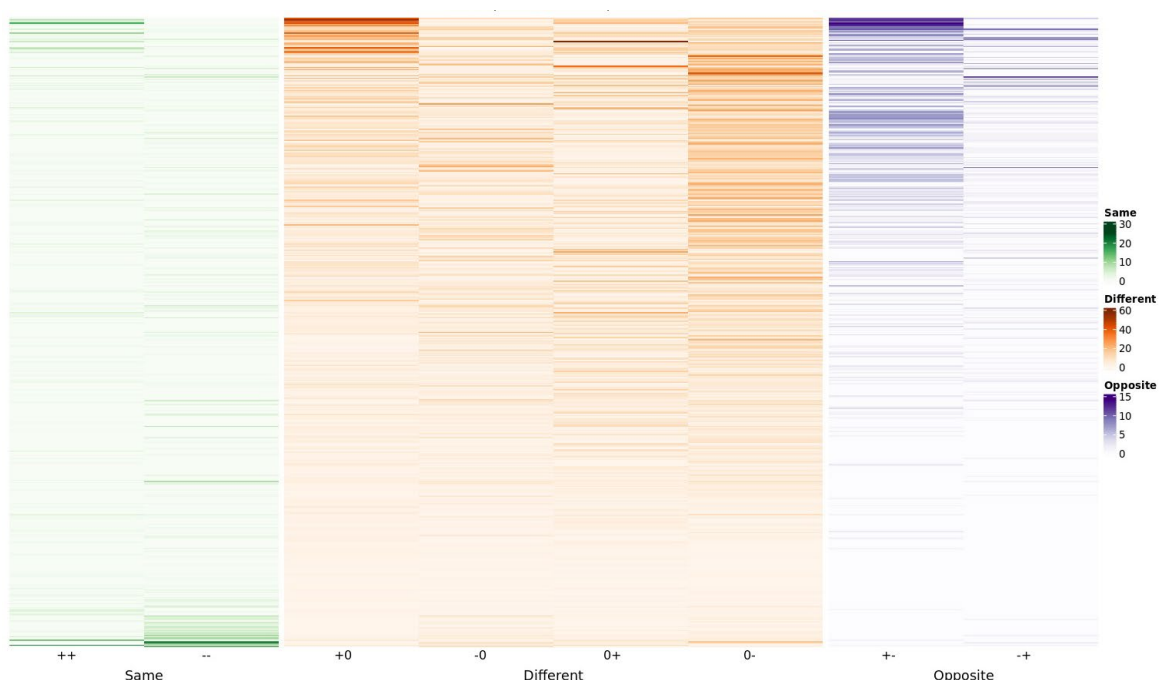
190 We employed this similarity measure to compare transcriptional patterns between females
191 and males, incorporating results across all APOE genotypes (e2x, e33, and e4x) and all cell
192 subclusters (**Figure 3A**). This allowed us to assess the consistency of sex-specific transcriptional
193 responses across AD and NCI samples. Next, we extended the analysis to genotype-based
194 comparisons, examining the similarity of transcriptional responses between APOE e2x and e33
195 carriers, as well as between e4x and e33 carriers (**Figure 3B, 3C**). For these analyses, we combined
196 results across sexes and cell subclusters to identify genotype-specific patterns of differential
197 expression.

198 To evaluate the effectiveness of the similarity metric, we plotted the expression patterns of
199 approximately 500 genes, sampled evenly across the range of similarity scores, incorporating
200 transcriptional changes associated with AD versus NCI across all APOE genotypes (e2x, e33, and
201 e4x) and cell clusters for both females and males (**Figure 4**). For each gene, we analyzed the
202 frequency of all possible combinations of expression patterns between females and males, such as
203 consistent upregulation, consistent downregulation, or divergent patterns. As shown in the plot,
204 genes with lower similarity scores are predominantly characterized by "opposite" and "different"
205 cases, indicating divergent transcriptional responses between sexes. In contrast, genes with higher
206 similarity scores tend to show more "same" direction cases, reflecting consistent transcriptional
207 changes between females and males. This analysis demonstrates that the similarity metric

208 effectively distinguishes shared versus divergent transcriptional patterns, supporting its utility in
209 identifying sex- and genotype-specific transcriptional responses in Alzheimer's disease.
210



211
212 **Figure 3. Distribution of similarity scores for different comparisons.** A) The distribution of
213 similarity scores for the comparison of females and males across all APOE genotypes (e2x, e33,
214 and e4x). B) The distribution of similarity scores for the comparison of APOE e2x and e33
215 genotypes across both sexes. C) The distribution of similarity scores for the comparison of APOE
216 e4x and e33 genotypes across both sexes.
217



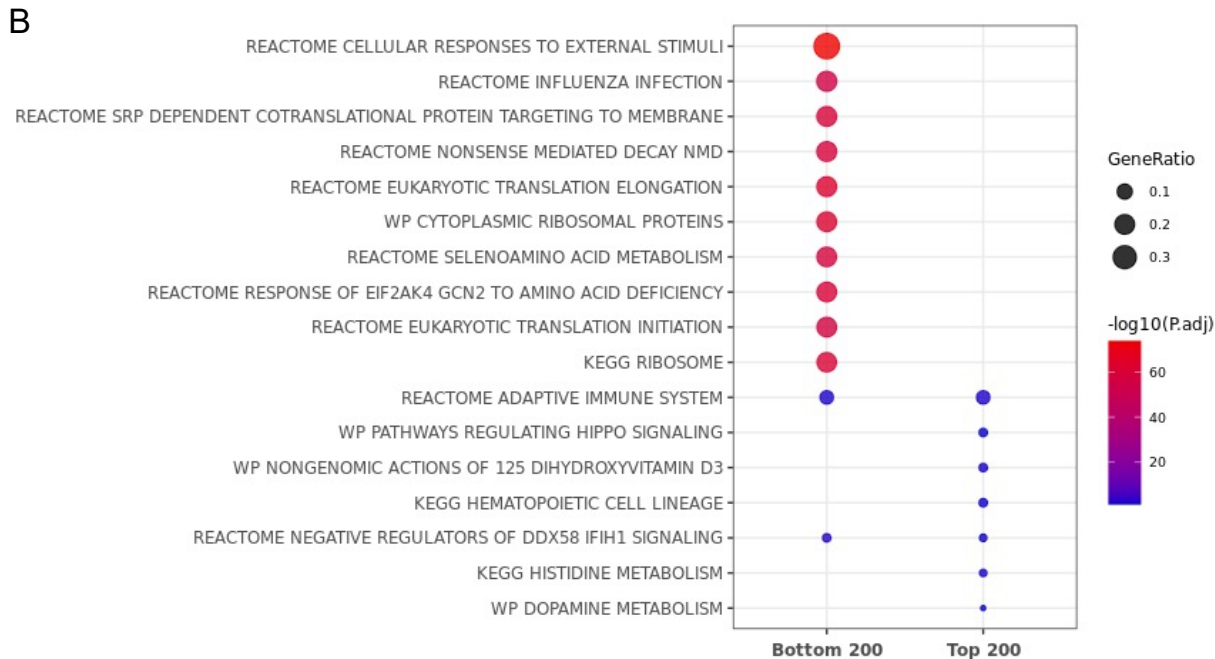
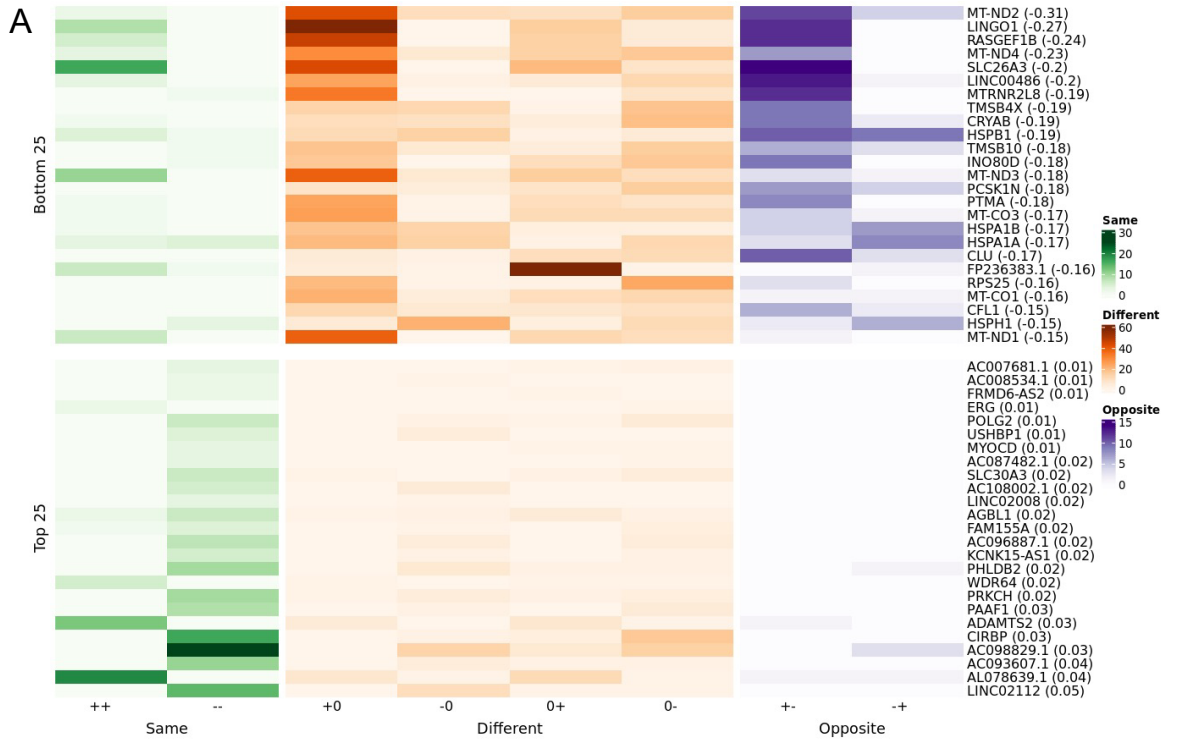
218

219 **Figure 4.** Heatmap illustrating the a set of approximately 500 genes that are evenly
220 distributed across the full range of similarity scores for the comparison of differential
221 expression patterns between females and males across all APOE genotypes. The heatmap
222 categorizes gene expression changes as "Same" (++, --), "Different" (+0, 0+, -0, 0-), or "Opposite"
223 (+-, -+), with color intensities indicating the number of occurrences across all cell subclusters.
224

225 Using the similarity score, we identified the top 25 (with the highest similarity) and bottom
226 25 (with the lowest similarity) genes for each of the three comparisons of our interest: sex
227 differences, *APOE* e2x vs e33, and *APOE* e4x vs e33. For sex differences, the bottom 25 genes
228 included *CLU* (Clusterin), a gene associated with AD risk and neuroinflammation, and *HSPB1*
229 (Heat Shock Protein Beta-1) which is associated with stress responses in neurodegeneration. Both
230 genes show divergent expression patterns between sexes (**Figure 5A**). Pathway enrichment
231 analysis of the top 200 and bottom 200 genes further revealed distinct biological processes
232 associated with shared and divergent transcriptional responses (**Figure 5B**). The top 200 genes,
233 enriched in pathways such as "dopamine metabolism" and "histidine metabolism" suggest
234 conserved roles in cellular metabolism, and hormone signaling across sexes. In contrast, the
235 bottom 200 genes, representing divergent transcriptional responses, were enriched in immune-
236 related and stress response pathways, including "cellular responses to external stimuli" "adaptive
237 immune system" and "nonsense-mediated decay". These enriched pathways point to sex-specific
238 differences in immune and stress-response mechanisms in AD, highlighting potential molecular
239 targets for understanding sex-related variability in disease progression.

240 For the comparison between *APOE* e2x and *APOE* e33 genotypes, the top 25 genes with
241 the highest similarity scores and the bottom 25 genes with the lowest similarity scores are shown
242 in **Figure 6A**. Pathway enrichment analysis revealed that the top 200 genes were enriched in
243 processes such as "fatty acid metabolism" and "SHC1 events in ERBB4 signaling," emphasizing
244 conserved roles in lipid metabolism and cellular signaling across these genotypes (**Figure 6B**).
245 Conversely, the bottom 200 genes were enriched in pathways associated with translational
246 regulation, such as "cytoplasmic ribosomal proteins" and "eukaryotic translation elongation," as
247 well as stress-response pathways like "cellular responses to external stimuli." These enrichments
248 highlight genotype-specific responses that may contribute to the differential impact of *APOE* e2
249 and *APOE* e33 in AD pathology. For the comparison between *APOE* e4x and *APOE* e33 genotypes,
250 the top 25 genes with the highest similarity scores and the bottom 25 genes with the lowest
251 similarity scores are shown in **Figure 7A**. Genes with the lowest similarity scores were enriched
252 in mitochondrial function and energy metabolism pathways, including "oxidative
253 phosphorylation" "electron transport chain" and "HSP90 chaperone cycle for steroid hormone
254 receptors" (**Figure 7B**). These results suggest that mitochondrial processes and stress response
255 pathways diverge significantly between *APOE* e4x and *APOE* e33 carriers.
256
257

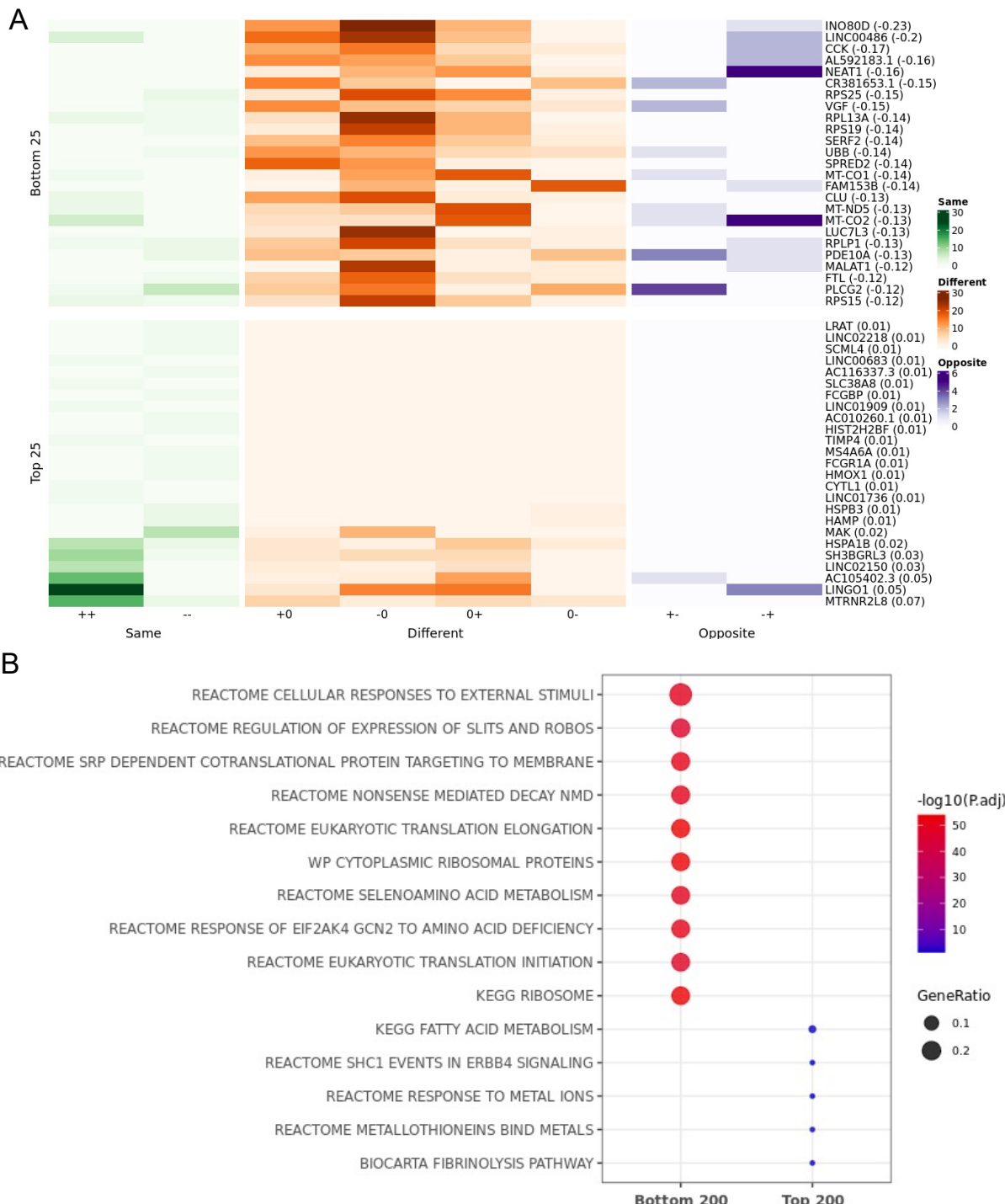
258



259

260 **Figure 5. The top 25 genes displaying the greatest and least differences between sexes across**
 261 **APOE genotypes and cell types. A)** Heatmap illustrating the top 25 and bottom 25 genes based
 262 on similarity scores for the comparison of differential expression patterns between females and
 263 males across all APOE genotypes and cell types. The heatmap categorizes gene expression
 264 changes as "Same" (++, --), "Different" (+0, 0+, -0, 0-), or "Opposite" (+-, -+), with color
 265 intensities indicating the number of occurrences across all cell subclusters. **B)** Pathway enrichment

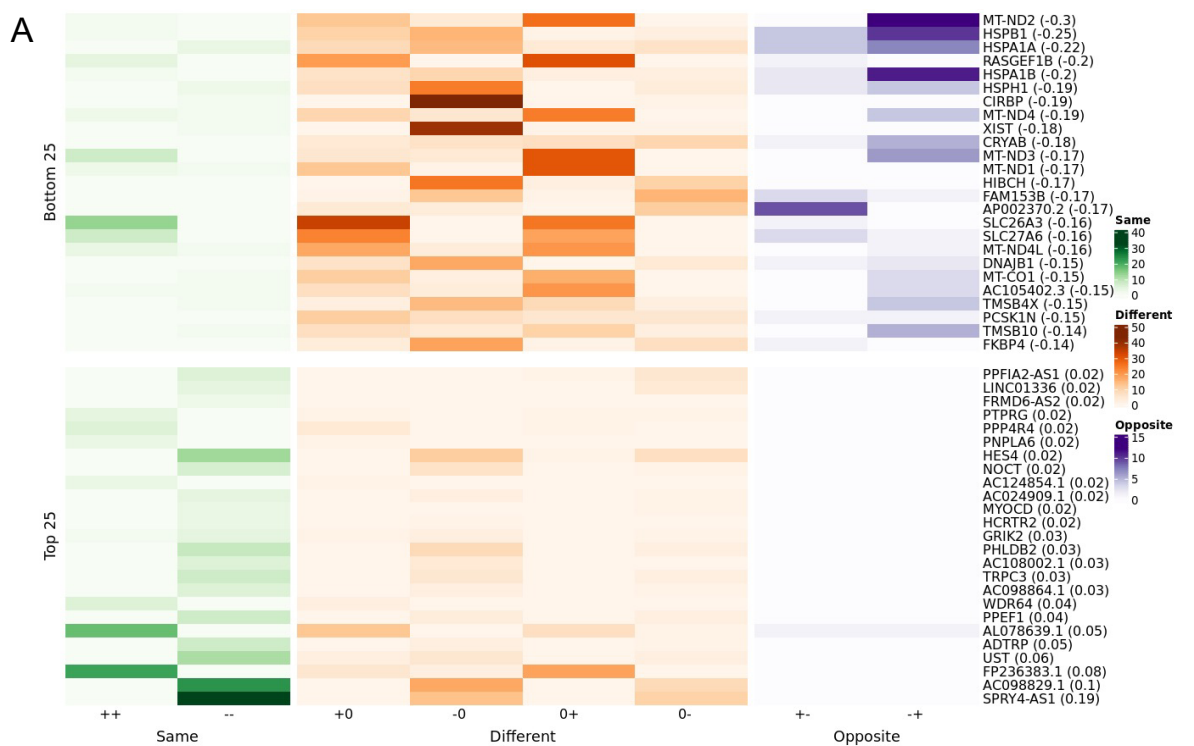
266 analysis for the top 200 and bottom 200 genes based on similarity scores in the comparison
 267 between females and males.



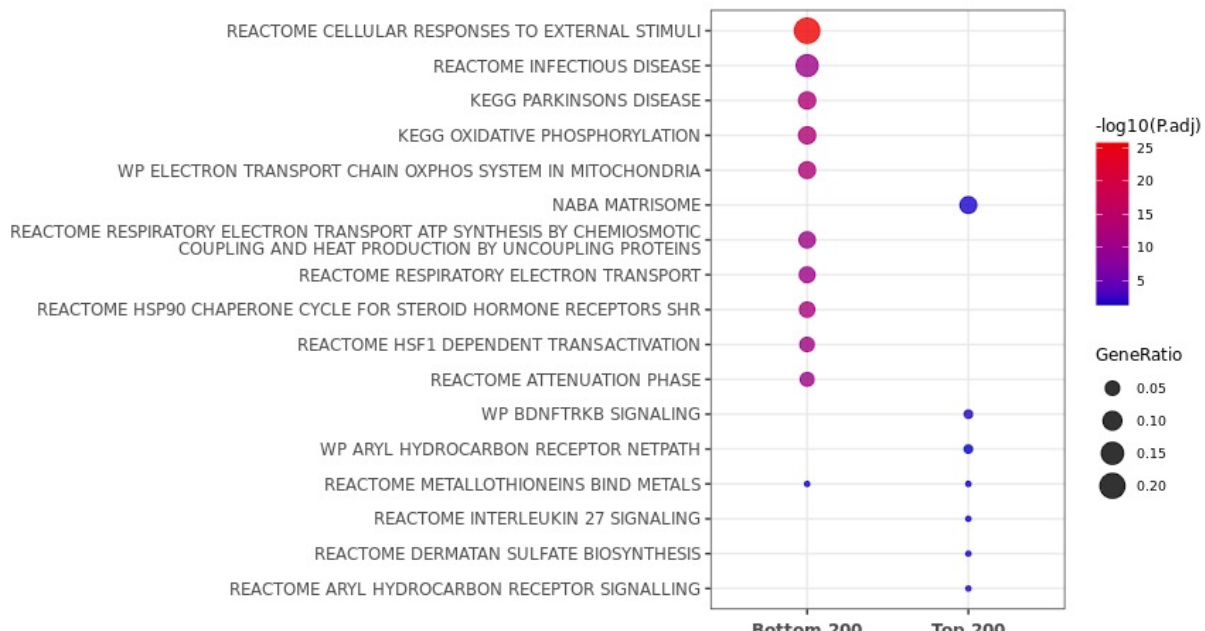
268

269 **Figure 6. The top 25 genes displaying the greatest and least differences between APOE e2x
 270 and e33 carriers across sexes and cell types. A)** Heatmap illustrating the top 25 and bottom 25
 271 genes based on similarity scores for the comparison of differential expression patterns between

272 APOE e2x and e33 carriers across sexes and cell types. The heatmap categorizes gene expression
 273 changes as "Same" (++, --), "Different" (+0, 0+, -0, 0-), or "Opposite" (+-, -+), with color
 274 intensities indicating the number of occurrences across all cell subclusters. **B)** Pathway enrichment
 275 analysis for the top 200 and bottom 200 genes based on similarity scores in the comparison
 276 between APOE e2x and e33 carriers.



B



278 **Figure 7. The top 25 genes displaying the greatest and least differences between APOE e4x**
279 **and e33 carriers across sexes and cell types. A)** Heatmap illustrating the top 25 and bottom 25
280 genes based on similarity scores for the comparison of differential expression patterns between
281 APOE e4x and e33 carriers across sexes and cell types. The heatmap categorizes gene expression
282 changes as "Same" (++, --), "Different" (+0, 0+, -0, 0-), or "Opposite" (+-, -+), with color
283 intensities indicating the number of occurrences across all cell subclusters. **B)** Pathway enrichment
284 analysis for the top 200 and bottom 200 genes based on similarity scores in the comparison
285 between APOE e4x and e33 carriers.

286 DISCUSSION

287 This study provides a comprehensive analysis of sex- and *APOE* genotype-specific transcriptional
288 changes in AD using a snRNA-seq dataset from the ROSMAP cohort. By performing differential
289 gene expression analysis across six stratified sex-*APOE* groups and applying a novel similarity
290 metric, Zhang-Yule similarity measure, for ternary vectors, we uncovered shared and divergent
291 transcriptional patterns across sexes and *APOE* genotypes. These findings highlight the interplay
292 between genetic risk, sex, and cell-type-specific transcriptional responses in AD pathophysiology.

293 Male *APOE* e2 carriers exhibited the highest number of DEGs when comparing AD to NCI
294 samples, suggesting a heightened transcriptional response in this subgroup. A majority of AD
295 signatures were identified in excitatory neurons, inhibitory neurons, astrocytes, oligodendrocyte
296 precursor cells, and one specific microglia cluster, highlighting the importance of these cell types
297 in transcriptional responses to AD across all sex-*APOE* groups. Conversely, several cell clusters,
298 including endothelial cells, CNS-associated macrophages (CAMs), pericytes, smooth muscle cells
299 (SMCs), and T cells, showed no significant transcriptional changes, indicating a limited or
300 negligible response to AD-related pathology in these populations.

301 In the comparison of transcriptional signatures across *APOE* genotypes in females, F_e4x
302 AD signatures were notably divergent from those of F_e2x and F_e33. This divergence was
303 particularly evident in comparisons such as F_e2x_AD vs. F_e2x_NCI and F_e4x_AD vs.
304 F_e4x_NCI, and F_e4x_AD vs. F_e4x_NCI and F_e33_AD vs. F_e33_NCI, which displayed a
305 higher number of DEGs that were unique to one condition. These unique DEGs suggest distinct
306 transcriptional responses in F_e4x carriers, aligning with the heightened AD risk associated with
307 *APOE* e4. Similarly, in males, M_e2x AD signatures were significantly divergent from M_e4x
308 and M_e33 AD signatures. These findings highlight the distinct transcriptional responses
309 associated with *APOE* e4 in females and *APOE* e2 in males, reflecting genotype-specific roles in
310 AD pathology.

311 The use of the Zhang-Yule similarity measure allowed us to quantify shared and divergent
312 transcriptional patterns across groups. Genes with high similarity scores represented conserved
313 transcriptional responses, reflecting core molecular processes shared across sexes and genotypes.
314 Conversely, genes with low similarity scores highlighted subgroup-specific pathways, particularly
315 in immune responses and stress-related mechanisms. These patterns reinforce the complexity of
316 AD pathology and emphasize the importance of examining both shared and divergent molecular
317 changes in understanding the disease.

318 Overall, this study highlights the intricate interplay of sex and *APOE* genotype in shaping
319 transcriptional responses in AD. By integrating cell-cluster-specific analyses with a similarity
320 scoring approach, we provide a detailed view of the molecular heterogeneity underlying AD. These
321 findings pave the way for future research to further elucidate the functional implications of

322 identified pathways and develop precision medicine strategies that address the diverse molecular
323 profiles of AD patients.

324

325 MATERIALS AND METHODS

326 To investigate the genes, pathways, and cell types underlying sex and *APOE* isoform differences
327 in AD pathology, we leveraged one of the most comprehensive single-nucleus RNA sequencing
328 (snRNA-seq) datasets in AD research by Mathys et al¹. This dataset includes 2.3 million nuclei
329 isolated from the prefrontal cortex of 427 participants in the ROSMAP cohort, spanning a wide
330 range of AD progression.

331 We used preprocessed read count data from the original study, which identified 54 high-
332 resolution cell types grouped into 12 major categories. These include 14 excitatory neuron
333 subtypes (Exc), 25 inhibitory neuron subtypes (Inh), oligodendrocytes (Oli), oligodendrocyte
334 precursor cells (OPCs), 3 astrocyte subtypes (Ast), and 5 immune cell types (microglia (Mic),
335 CNS-associated macrophages (CAMs), and T cells). The dataset also encompasses several
336 vascular cell types, including endothelial cells (End), smooth muscle cells (SMCs), fibroblasts
337 (Fib), and pericytes (Per).

338 Cell cluster specific differential expression analysis

339 Differential expression analysis was performed for each sex-*APOE* group, including F_e2x,
340 F_e33, F_e4x, M_e2x, M_e33, and M_e4x, comparing individuals with Alzheimer's disease (AD)
341 to control samples with no cognitive impairment (NCI). This analysis was conducted at the cell-
342 cluster level to account for cell-type-specific transcriptional changes. We utilized the FindMarkers
343 function in Seurat version 5 for cluster-specific DEG identification. Genes were included in the
344 analysis if they were expressed in at least 10% of the cells in either group (min.pct = 0.1). To adjust
345 for potential confounding factors, we incorporated covariates including nCount_RNA (total RNA
346 counts), post-mortem interval (PMI), and age at death. The Benjamini-Hochberg (BH) method was
347 used to adjust p-values for multiple testing. Significant differentially expressed genes (DEGs) were
348 defined as those meeting the following thresholds: adjusted p-value (adj.p) < 0.05 and absolute
349 fold change (|FC|) > 1.3. Filtered genes that passed these criteria were included in downstream
350 analyses. Enrichment analysis was performed by using R package GTest (V1.0.9).

351

352 Similarity measure for evaluating similarity of transcriptional patterns between sex and 353 *APOE* genotype subgroups

354 To quantitatively evaluate the similarity of differential expression patterns across sexes and
355 *APOE* genotypes, we developed and applied a novel similarity measure termed Zhang-Yu
356 similarity measure. This similarity measure calculates the similarity between two N-dimensional
357 ternary vectors, i.e., *X* and *Y*, representing differential expression statuses (AD versus NCI) of the
358 genes in two different groups. In a ternary vector where each element takes three discrete values
359 including -1, 0 and 1, each dimension represents the differential expression status of a gene as
360 either up-regulation (+1), down-regulation (-1), or no significant change (0). The similarity score
361 for two ternary vectors is defined as:

362

363
$$Score = \frac{(S_{11} + S_{(-1)(-1)}) - 0.5 * (S_{10} + S_{(-1)0} + S_{01} + S_{0(-1)}) - (S_{1(-1)} + S_{(-1)1})}{N}$$

364 where, S_{ij} represents the number of occurrences of $X(k) = i$ and $Y(k) = j$, where $k=1, \dots, N$.
365 Therefore S_{11} represents for the number of the up-regulation matches in both groups, $S_{(-1)(-1)}$ for the
366 number of the down-regulation matches in both groups, and S_{10} for the number of mismatches with
367 the upregulation in X and no change in Y , and so on so forth. N is the number of genes evaluated
368 in the differential expression analysis.

369 We applied this similarity measure to three key comparisons:

370 1. **Female vs. Male (F vs. M):**

- 371 ○ **X:** Differential expression results ($\{-1,0,1\}$) for females across all cell clusters
372 and *APOE* genotypes: F_e2x_AD vs. F_e2x_NCI, F_e33_AD vs. F_e33_NCI,
373 and F_e4x_AD vs. F_e4x_NCI.
- 374 ○ **Y:** Differential expression results ($\{-1,0,1\}$) for males across all cell clusters and
375 *APOE* genotypes: M_e2x_AD vs. M_e2x_NCI, M_e33_AD vs. M_e33_NCI, and
376 M_e4x_AD vs. M_e4x_NCI.
- 377 ○ **N:** Total number of cell clusters (54) multiplied by 3 comparisons = 162.

378 2. ***APOE* e2x vs. e33:**

- 379 ○ **X:** Differential expression results ($\{-1,0,1\}$) across all cell clusters for *APOE* e2x:
380 F_e2x_AD vs. F_e2x_NCI and M_e2x_AD vs. M_e2x_NCI.
- 381 ○ **Y:** Differential expression results ($\{-1,0,1\}$) across all cell clusters for *APOE* e33:
382 F_e33_AD vs. F_e33_NCI and M_e33_AD vs. M_e33_NCI.
- 383 ○ **N:** Total number of cell clusters (54) multiplied by 2 comparisons = 108.

384 3. ***APOE* e4x vs. e33:**

- 385 ○ **X:** Differential expression results ($\{-1,0,1\}$) across all cell clusters for *APOE* e4x:
386 F_e4x_AD vs. F_e4x_NCI and M_e4x_AD vs. M_e4x_NCI.
- 387 ○ **Y:** Differential expression results ($\{-1,0,1\}$) across all cell clusters for *APOE* e33:
388 F_e33_AD vs. F_e33_NCI and M_e33_AD vs. M_e33_NCI.
- 389 ○ **N:** Total number of cell clusters (54) multiplied by 2 comparisons = 108.

390

391 **CONFLICT OF INTEREST STATEMENT**

392 All authors declared no conflict of interest.

393

394 **FUNDING**

395 This work was supported in part by funding from NIH RF1 (RF1AG054014), R56 (R56AG058655)
396 and RF1 (RF1AG074010) to DC and BZ, NIH U01 (UO1AG046170), RF1 (RF1AG057440),
397 RO1(RO1AG057907) to BZ.

398

399

400

401 **References**

- 402 1. Karantzoulis, S.; Galvin, J. E., Distinguishing Alzheimer's disease from other major
403 forms of dementia. *Expert Rev Neurother* **2011**, *11* (11), 1579-91.
- 404 2. 2020 Alzheimer's disease facts and figures. *Alzheimers Dement* **2020**.
- 405 3. Barnes, L. L.; Wilson, R. S.; Schneider, J. A.; Bienias, J. L.; Evans, D. A.; Bennett, D.
406 A., Gender, cognitive decline, and risk of AD in older persons. *Neurology* **2003**, *60* (11), 1777-
407 81.
- 408 4. Edland, S. D.; Rocca, W. A.; Petersen, R. C.; Cha, R. H.; Kokmen, E., Dementia and
409 Alzheimer disease incidence rates do not vary by sex in Rochester, Minn. *Archives of neurology*
410 **2002**, *59* (10), 1589-93.
- 411 5. Kawas, C.; Gray, S.; Brookmeyer, R.; Fozard, J.; Zonderman, A., Age-specific
412 incidence rates of Alzheimer's disease: the Baltimore Longitudinal Study of Aging. *Neurology*
413 **2000**, *54* (11), 2072-7.
- 414 6. Plassman, B. L.; Langa, K. M.; McCammon, R. J.; Fisher, G. G.; Potter, G. G.; Burke,
415 J. R.; Steffens, D. C.; Foster, N. L.; Giordani, B.; Unverzagt, F. W.; Welsh-Bohmer, K. A.;
416 Heeringa, S. G.; Weir, D. R.; Wallace, R. B., Incidence of dementia and cognitive impairment,
417 not dementia in the United States. *Annals of neurology* **2011**, *70* (3), 418-26.
- 418 7. Seshadri, S.; Wolf, P. A.; Beiser, A.; Au, R.; McNulty, K.; White, R.; D'Agostino, R.
419 B., Lifetime risk of dementia and Alzheimer's disease. The impact of mortality on risk estimates
420 in the Framingham Study. *Neurology* **1997**, *49* (6), 1498-504.
- 421 8. Hua, X.; Hibar, D. P.; Lee, S.; Toga, A. W.; Jack, C. R., Jr.; Weiner, M. W.;
422 Thompson, P. M.; Alzheimer's Disease Neuroimaging, I., Sex and age differences in atrophic
423 rates: an ADNI study with n=1368 MRI scans. *Neurobiology of aging* **2010**, *31* (8), 1463-80.
- 424 9. Skup, M.; Zhu, H.; Wang, Y.; Giovanello, K. S.; Lin, J. A.; Shen, D.; Shi, F.; Gao,
425 W.; Lin, W.; Fan, Y.; Zhang, H.; Alzheimer's Disease Neuroimaging, I., Sex differences in
426 grey matter atrophy patterns among AD and aMCI patients: results from ADNI. *NeuroImage*
427 **2011**, *56* (3), 890-906.
- 428 10. Ardekani, B. A.; Convit, A.; Bachman, A. H., Analysis of the MIRIAD Data Shows Sex
429 Differences in Hippocampal Atrophy Progression. *Journal of Alzheimer's disease : JAD* **2016**, *50*
430 (3), 847-57.
- 431 11. Mayeux, R., Epidemiology of neurodegeneration. *Annu Rev Neurosci* **2003**, *26*, 81-104.
- 432 12. Farrer, L. A.; Cupples, L. A.; Haines, J. L.; Hyman, B.; Kukull, W. A.; Mayeux, R.;
433 Myers, R. H.; Pericak-Vance, M. A.; Risch, N.; van Duijn, C. M., Effects of age, sex, and
434 ethnicity on the association between apolipoprotein E genotype and Alzheimer disease. A meta-
435 analysis. APOE and Alzheimer Disease Meta Analysis Consortium. *Jama* **1997**, *278* (16), 1349-
436 56.
- 437 13. Neu, S. C.; Pa, J.; Kukull, W.; Beekly, D.; Kuzma, A.; Gangadharan, P.; Wang, L. S.;
438 Romero, K.; Arneric, S. P.; Redolfi, A.; Orlandi, D.; Frisoni, G. B.; Au, R.; Devine, S.;
439 Auerbach, S.; Espinosa, A.; Boada, M.; Ruiz, A.; Johnson, S. C.; Kosik, R.; Wang, J. J.;
440 Hsu, W. C.; Chen, Y. L.; Toga, A. W., Apolipoprotein E Genotype and Sex Risk Factors for
441 Alzheimer Disease: A Meta-analysis. *JAMA neurology* **2017**, *74* (10), 1178-1189.
- 442 14. Altmann, A.; Tian, L.; Henderson, V. W.; Greicius, M. D.; Alzheimer's Disease
443 Neuroimaging Initiative, I., Sex modifies the APOE-related risk of developing Alzheimer
444 disease. *Annals of neurology* **2014**, *75* (4), 563-73.
- 445 15. Hohman, T. J.; Dumitrescu, L.; Barnes, L. L.; Thambisetty, M.; Beecham, G.; Kunkle,
446 B.; Gifford, K. A.; Bush, W. S.; Chibnik, L. B.; Mukherjee, S.; De Jager, P. L.; Kukull, W.;

- 447 Crane, P. K.; Resnick, S. M.; Keene, C. D.; Montine, T. J.; Schellenberg, G. D.; Haines, J. L.;
448 Zetterberg, H.; Blennow, K.; Larson, E. B.; Johnson, S. C.; Albert, M.; Bennett, D. A.;
449 Schneider, J. A.; Jefferson, A. L.; Alzheimer's Disease Genetics, C.; the Alzheimer's Disease
450 Neuroimaging, I., Sex-Specific Association of Apolipoprotein E With Cerebrospinal Fluid
451 Levels of Tau. *JAMA neurology* **2018**, *75* (8), 989-998.
- 452 16. Cavedo, E.; Chiesa, P. A.; Houot, M.; Ferretti, M. T.; Grothe, M. J.; Teipel, S. J.;
453 Lista, S.; Habert, M. O.; Potier, M. C.; Dubois, B.; Hampel, H.; Group, I. N.-p. S.; Alzheimer
454 Precision Medicine, I., Sex differences in functional and molecular neuroimaging biomarkers of
455 Alzheimer's disease in cognitively normal older adults with subjective memory complaints.
Alzheimer's & dementia : the journal of the Alzheimer's Association **2018**, *14* (9), 1204-1215.
- 456 17. Sampedro, F.; Vilaplana, E.; de Leon, M. J.; Alcolea, D.; Pegueroles, J.; Montal, V.;
457 Carmona-Iragui, M.; Sala, I.; Sanchez-Saudinos, M. B.; Anton-Aguirre, S.; Morenas-
458 Rodriguez, E.; Camacho, V.; Falcon, C.; Pavia, J.; Ros, D.; Clarimon, J.; Blesa, R.; Lleo, A.;
459 Fortea, J.; Alzheimer's Disease Neuroimaging, I., APOE-by-sex interactions on brain structure
460 and metabolism in healthy elderly controls. *Oncotarget* **2015**, *6* (29), 26663-74.
- 461 18. Sundermann, E. E.; Tran, M.; Maki, P. M.; Bondi, M. W., Sex differences in the
462 association between apolipoprotein E epsilon4 allele and Alzheimer's disease markers.
Alzheimers Dement (Amst) **2018**, *10*, 438-447.
- 463 19. Kim, J.; Fischer, C. E.; Schweizer, T. A.; Munoz, D. G., Gender and Pathology-Specific
464 Effect of Apolipoprotein E Genotype on Psychosis in Alzheimer's Disease. *Current Alzheimer
465 research* **2017**, *14* (8), 834-840.
- 466 20. Xing, Y.; Qin, W.; Li, F.; Jia, X. F.; Jia, J., Apolipoprotein E epsilon4 status modifies
467 the effects of sex hormones on neuropsychiatric symptoms of Alzheimer's disease. *Dementia and
468 geriatric cognitive disorders* **2012**, *33* (1), 35-42.
- 469 21. Shinohara, M.; Murray, M. E.; Frank, R. D.; Shinohara, M.; DeTure, M.; Yamazaki,
470 Y.; Tachibana, M.; Atagi, Y.; Davis, M. D.; Liu, C. C.; Zhao, N.; Painter, M. M.; Petersen,
471 R. C.; Fryer, J. D.; Crook, J. E.; Dickson, D. W.; Bu, G.; Kanekiyo, T., Impact of sex and
472 APOE4 on cerebral amyloid angiopathy in Alzheimer's disease. *Acta neuropathologica* **2016**,
473 *132* (2), 225-34.
- 474 22. Guo, L.; Cao, J.; Hou, J.; Li, Y.; Huang, M.; Zhu, L.; Zhang, L.; Lee, Y.; Duarte, M.
475 L.; Zhou, X.; Wang, M.; Liu, C. C.; Martens, Y.; Chao, M.; Goate, A.; Bu, G.; Haroutunian,
476 V.; Cai, D.; Zhang, B., Sex specific molecular networks and key drivers of Alzheimer's disease.
Molecular neurodegeneration **2023**, *18* (1), 39.
- 477 23. Wang, M.; Roussos, P.; McKenzie, A.; Zhou, X.; Kajiwara, Y.; Brennand, K. J.; De
478 Luca, G. C.; Crary, J. F.; Casaccia, P.; Buxbaum, J. D.; Ehrlich, M.; Gandy, S.; Goate, A.;
479 Katsel, P.; Schadt, E.; Haroutunian, V.; Zhang, B., Integrative network analysis of nineteen
480 brain regions identifies molecular signatures and networks underlying selective regional
481 vulnerability to Alzheimer's disease. *Genome Med* **2016**, *8* (1), 104.
- 482 24. De Jager, P. L.; Ma, Y.; McCabe, C.; Xu, J.; Vardarajan, B. N.; Felsky, D.; Klein, H.
483 U.; White, C. C.; Peters, M. A.; Lodgson, B.; Nejad, P.; Tang, A.; Mangravite, L. M.; Yu,
484 L.; Gaiteri, C.; Mostafavi, S.; Schneider, J. A.; Bennett, D. A., A multi-omic atlas of the human
485 frontal cortex for aging and Alzheimer's disease research. *Sci Data* **2018**, *5*, 180142.
- 486 25. Mathys, H.; Peng, Z.; Boix, C. A.; Victor, M. B.; Leary, N.; Babu, S.; Abdelhady, G.;
487 Jiang, X.; Ng, A. P.; Ghafari, K.; Kunisky, A. K.; Mantero, J.; Galani, K.; Lohia, V. N.;
488 Fortier, G. E.; Lotfi, Y.; Ivey, J.; Brown, H. P.; Patel, P. R.; Chakraborty, N.; Beaudway, J.
489 I.; Imhoff, E. J.; Keeler, C. F.; McChesney, M. M.; Patel, H. H.; Patel, S. P.; Thai, M. T.;

493 Bennett, D. A.; Kellis, M.; Tsai, L. H., Single-cell atlas reveals correlates of high cognitive
494 function, dementia, and resilience to Alzheimer's disease pathology. *Cell* **2023**, *186* (20), 4365-
495 4385 e27.
496